

Entropy production by resonance decays

TPR 96-09, DUKE-TH-96-117

Stefan Ochs

Institut für Theoretische Physik, Universität Regensburg, D-93040 Regensburg, Germany

Ulrich Heinz*

Physics Department, Duke University, Durham, NC 27708-0305, USA

February 1, 2008

Abstract

We investigate entropy production for an expanding system of particles and resonances with isospin symmetry – in our case pions and ρ mesons – within the framework of relativistic kinetic theory. A cascade code to simulate the kinetic equations is developed and results for entropy production and particle spectra are presented.

1 Introduction

The search for the Quark-Gluon-Plasma (QGP) requires a detailed and quantitative understanding of the influence of known physics on the particle spectra and abundances from heavy ion collisions, such that possible systematic deviations due to the new physics of the QGP can be recognized in the experimental data.

When interpreting the pion momentum spectra [1]-[6] the question of entropy production during freeze-out occurred [7]. If the contribution to entropy production after freeze-out due to resonance decays is known, the entropy of the system before freeze-out can be calculated by measuring the multiplicities and momentum spectra of all particles after freeze-out and combining these data with an estimate of their initial spatial distribution (e.g. from a fireball model). It is then crucial to know how much entropy is produced in an expanding system during the transition (freeze-out) from a highly interacting (equilibrium) state to a non-interacting one. Here we will give such an estimate for a simple system of pions and ρ mesons, using the framework of relativistic kinetic theory [8]. This will enable us to estimate the reliability of models based on hydrodynamics in which freeze-out is usually implemented by cutting off the entropy-conserving expansion sharply at the so-called freeze-out surface, neglecting possible entropy production during the decoupling process or afterwards by the decay of unstable resonances.

The paper is organized as follows: In Section 2 we will formulate via relativistic kinetic theory the problem of resonance formation and decay for a system of pions and ρ mesons, including Bose statistical effects. We will show that the collision term satisfies Boltzmann's H-theorem and discuss the formation and decay rates for ρ mesons. In Section 3 we describe a simulation of the kinetic equations of our system with the help of a cascade code, and in Section 4 we present our results, in particular on the production of entropy by resonance formation and decays. We will also discuss the influence of the interplay between ρ -formation and -decay on the time evolution of the particle spectra. In Section 5 we summarize our results. Some technical details are given in the Appendix.

In the following we will use natural units, $\hbar = c = k_B = 1$, if not stated explicitly otherwise.

2 Kinetic theory for the π - ρ -system

As a starting point we consider the kinetic equation

$$m \frac{d}{dt} f(x, p) = -\Gamma_{\text{loss}}(x, p) f(x, p) + \Gamma_{\text{gain}}(x, p) (1 + f(x, p)), \quad (1)$$

*On sabbatical leave from Institut für Theoretische Physik, Universität Regensburg, D-93040 Regensburg, Germany.

where τ is the proper-time of a particle at point x with momentum p , and the right hand side of Eq. (1) is the collision term. The latter consists of a term for particle loss (with rate Γ_{loss}) and one for particle gain (with rate Γ_{gain}). A vanishing collision term means vanishing entropy production (Liouville theorem). The left hand side of the kinetic equation can be rewritten as

$$m \frac{d}{d\tau} = \left(m \frac{dx^\mu}{d\tau} \right) \frac{\partial}{\partial x^\mu} + \left(m \frac{dp^\mu}{d\tau} \right) \frac{\partial}{\partial p^\mu} = p^\mu \frac{\partial}{\partial x^\mu} + F^\mu \frac{\partial}{\partial p^\mu}. \quad (2)$$

In the following we neglect external or mean-field forces by setting F^μ to zero.

For $2 \rightarrow 2$ processes Boltzmann's H-theorem can be proven from unitarity and particle number conservation alone [8] whereas in $2 \rightleftharpoons 1$ reactions as in resonance formation and decay a different approach has to be taken. In [9] the bilateral normalization condition was exploited. We will here consider the isospin symmetry of the matrix elements to evaluate the gain and loss rates for the π - ρ -system and thus prove the Boltzmann H-theorem explicitly.

At low relative momentum the $\pi\pi$ interaction is dominated by the ρ resonance, with a small non-resonant background [10]. We are interested in the very last stage of a nuclear collision, after the pions and ρ mesons have “frozen out”, i.e. stopped interacting with other particles and with each other. After this freeze-out we expect the dominant physical process to be the decay of the unstable ρ mesons which we want to describe by kinetic theory. But in order for such a description to be consistent and the calculation of entropy production to be meaningful, our collision term should allow for detailed balance, which implies that we also have to include the inverse process $\pi\pi \rightarrow \rho$ (resonant $\pi\pi$ scattering), however small its rate should be.

The interaction Hamiltonian for the π - ρ -system is of the form [10]

$$H_{\text{int}} = f_{\rho\pi\pi} \vec{\rho}^\mu (\vec{\varphi} \times \partial_\mu \vec{\varphi}), \quad (3)$$

where the vectors refer to the isospin structure, and $\vec{\rho}^\mu$ is a massive spin-1 vector field satisfying the gauge condition

$$\partial_\mu \vec{\rho}^\mu = 0. \quad (4)$$

Due to energy momentum conservation and isospin symmetry only the processes $\rho^\alpha \leftrightarrow \pi^\beta \pi^\gamma$ are allowed where $\alpha, \beta, \gamma \in \{0, +, -\}$ are pairwise different.

To write down the rates in terms of the distribution functions, we assume that the ensemble averages of multiple products of creation and annihilation operators arising from treating H_{int} in first order perturbation theory can be factorized into products of ensemble averages of 1-particle operators, given by the following replacement (for ρ mesons α is a double index denoting both the spin and isospin component of the particle):

$$\langle a^{\alpha\dagger}(k) a^{\alpha'}(k') \rangle = \delta(\vec{k} - \vec{k}') f_\alpha(k) \delta^{\alpha\alpha'} \quad (5)$$

$$\langle a^\alpha(k) a^{\alpha'\dagger}(k') \rangle = \delta(\vec{k} - \vec{k}') (1 + f_\alpha(k)) \delta^{\alpha\alpha'} \quad (6)$$

$$\langle a^\alpha(k) a^{\alpha'}(k') \rangle = \langle a^{\alpha\dagger}(k) a^{\alpha'\dagger}(k') \rangle = 0. \quad (7)$$

In global thermal equilibrium this is justified by the thermal Wick theorem [11], and in [12] it was shown how to generalize the latter to local thermal equilibrium systems. For non-equilibrium ensembles the validity of this ansatz has been proven from first principles only for the ϕ^4 -theory [13]. We use it here because it leads to the classically expected result.

Let us now introduce pion and ρ meson distribution functions $f_\alpha \equiv f_{\pi\alpha}$ and $F_\alpha \equiv f_{\rho\alpha}$. In the case of the ρ , F_α describes a single isospin *and* spin projection, but we assume spin saturation such that the distribution functions for the three spin projections are equal, and therefore suppress the spin index on F_α . The loss rates are then given by

$$\Gamma_{\text{loss}}^{\pi^\alpha}(p_1) = (2\pi)^4 f_{\rho\pi\pi}^2 \sum_{\beta, \gamma} |\varepsilon_{\alpha\beta\gamma}| \int Dp_2 Dp_3 (\mathcal{M}(p_1, p_3) + \mathcal{M}(p_2, p_3)) f_\beta(p_2) (1 + F_{-\gamma}(p_3)) \delta(p_1 + p_2 - p_3), \quad (8)$$

$$\Gamma_{\text{loss}}^{\rho^\alpha}(p_3) = (2\pi)^4 \frac{f_{\rho\pi\pi}^2}{s_\rho(s_\rho + 1)} \sum_{\beta, \gamma} |\varepsilon_{\alpha\beta\gamma}| \int Dp_1 Dp_2 \mathcal{M}(p_1, p_3) (1 + f_{-\beta}(p_1)) (1 + f_{-\gamma}(p_2)) \delta(p_1 + p_2 - p_3), \quad (9)$$

while the gain rates are simply given by replacing $f_\alpha \leftrightarrow 1 + f_\alpha$ and $F_\alpha \leftrightarrow 1 + F_\alpha$. Here $\varepsilon_{\alpha\beta\gamma}$ is the totally antisymmetric tensor, Dp is the Lorentz-invariant measure in momentum space

$$Dp := \frac{d^4 p}{(2\pi)^4} 2\pi \delta(p^2 - m^2) \Theta(p_0) = \frac{1}{(2\pi)^3} \frac{d^3 p}{2E}, \quad (10)$$

where $E = \sqrt{\vec{p}^2 + m^2}$, and the distribution functions are always taken on the mass-shell.

The two contributions to the pion loss term in Eq. (8) arise from the two possibilities in (3) to let the derivative act on either one of the two scattering pions.

The momentum dependent part of the matrix element as obtained from (3) in first order perturbation theory is given by

$$\mathcal{M}(p_i, p_\rho) = -p_i^2 + \frac{(p_i p_\rho)^2}{m_\rho^2} = \frac{1}{m_\rho^2} \left(\frac{1}{4} ((p_i \pm p_\rho)^2 - p_i^2 - p_\rho^2)^2 - p_i^2 m_\rho^2 \right). \quad (11)$$

Here we have already summed over the three spin states of the ρ . To describe a single ρ spin state in a spin saturated system, Eqs. (11) and (12) below must be multiplied by a factor $1/s_\rho(s_\rho + 1) = 1/3$, as in Eq. (9). Since in Eq. (8) this factor is missing, this rate contains already the sum over all final ρ spin states.

The dependence of the matrix element on the pion momentum p_i arises from the derivative in the $\rho\pi\pi$ -coupling (3), whereas the one on $p_3 = p_\rho$ comes from the ρ -polarization tensor [14] which appears after summing over all three spin states. If the meson masses for different isospin states are taken to be equal, (11) can be simplified by using the momentum conserving δ -functions in (8,9) to evaluate $p_i \pm p_j$ and exploiting the mass-shell conditions $p_i^2 = m_i^2$:

$$\mathcal{M}(p_1, p_3) = \mathcal{M}(p_2, p_3) = \frac{1}{4} (m_\rho^2 - (2m_\pi)^2). \quad (12)$$

In this case the two contributions to the loss rate in (8) become equal.

In kinetic theory the entropy current for bosons or fermions is given by

$$S_\mu(x) = - \sum_i \int Dp p_\mu \left[f_i(x, p) \ln f_i(x, p) \mp (1 \pm f_i(x, p)) \ln(1 \pm f_i(x, p)) \right. \\ \left. + \bar{f}_i(x, p) \ln \bar{f}_i(x, p) \mp (1 \pm \bar{f}_i(x, p)) \ln(1 \pm \bar{f}_i(x, p)) \right], \quad (13)$$

with the upper (lower) sign for bosons (fermions). The rate of entropy production can then be written as

$$\partial^\mu S_\mu = - \sum_i \int Dp \left[(p_\mu \partial^\mu f_i(x, p)) \ln \left(\frac{f_i(x, p)}{1 \pm f_i(x, p)} \right) + (p_\mu \partial^\mu \bar{f}_i(x, p)) \ln \left(\frac{\bar{f}_i(x, p)}{1 \pm \bar{f}_i(x, p)} \right) \right]. \quad (14)$$

In our π - ρ -system all particles are bosons, i.e. the plus signs apply and there are no anti-particle contributions. The sum over i in (14) goes over the three charge states of the pions and ρ mesons and additionally over the three spin projections of the latter. After replacing $p_\mu \partial^\mu f(x, p)$ in (14) by the r.h.s. of the kinetic equation (1), the sum over the three ρ spin states cancels the factor $1/s_\rho(s_\rho + 1)$ in Eq. (9), and one gets, after some renaming of integration variables and permutation of the isospin indices α, β, γ ,

$$\partial^\mu S_\mu = (2\pi)^4 f_{\rho\pi\pi}^2 \sum_{\alpha\beta\gamma} |\varepsilon_{\alpha\beta\gamma}| \int Dp_1 Dp_2 Dp_3 \mathcal{M}(p_1, p_3) \delta(p_1 + p_2 - p_3) \\ \times (1 + f_\alpha(p_1))(1 + f_\beta(p_2)) F_{-\gamma}(p_3) (y - 1) \ln y, \quad (15)$$

where

$$y = \frac{f_\alpha(p_1)f_\beta(p_2)(1 + F_{-\gamma}(p_3))}{(1 + f_\alpha(p_1))(1 + f_\beta(p_2))F_{-\gamma}(p_3)}. \quad (16)$$

y and \mathcal{M} are positive by definition. Since for $y \geq 0$ the expression $(y - 1) \ln y$ is positive semidefinite, we have $\partial^\mu S_\mu \geq 0$ always. This proves the Boltzmann H-theorem in our case and for similar systems with symmetric isospin structure. The collision integral (15) vanishes only if $y = 1$.

Expressing (similarly to Eq. (13)) the isospin current and the energy momentum tensor through the distribution functions $f_i(x, p)$ [15], one can use the conservation laws for these quantities together with the condition for vanishing entropy production, $y = 1$, to derive the local equilibrium Bose distribution

$$\frac{f_i(x, p_i)}{1 + f_i(x, p_i)} = \exp\left(-[\mu(x)q_i + u_\nu(x)p_i^\nu]/T(x)\right) \quad \text{or} \quad f_i(x, p_i) = \frac{1}{e^{[\mu(x)q_i + u_\nu(x)p_i^\nu]/T(x)} - 1}, \quad (17)$$

where $q_i = 0, \pm 1$ is the electric charge of species i .

Important for a simulation of the kinetic equations will be the decay rate of the ρ meson. In the rest frame of a ρ with a given spin polarization it can be cast in the form

$$\Gamma_{\text{loss}}^{\rho\alpha}(m_\rho) = \underbrace{\frac{f_{\rho\pi\pi}^2}{16\pi s_\rho(s_\rho + 1)} \frac{(m_\rho^2 - (2m_\pi)^2)^{3/2}}{m_\rho}}_{\text{free decay rate } \Gamma_{\text{free}}} \cdot \frac{|\varepsilon_{\alpha\beta\gamma}|}{2} \int d(\cos \theta) (1 + f_\beta(\vec{p})) (1 + f_\gamma(-\vec{p})). \quad (18)$$

The prefactor is the free decay rate Γ_{free} , and the integral over the pion emission angles relative to the velocity of the ρ in the local heat bath gives the medium corrections due to Bose stimulated decay. The pion distribution functions under the integral are evaluated at $|p| = \sqrt{m_\rho^2 - 4m_\pi^2}$, the pion momentum in the rest frame of the decaying ρ meson.

In the limit of free decay in the vacuum the kinetic equation for ρ mesons takes the following simple form

$$E_\rho \frac{d}{dt} F_\alpha(p_\rho, t) = -\Gamma_{\text{free}} F_\alpha(p_\rho, t). \quad (19)$$

This is solved by

$$F_\alpha(p_\rho, t) = F_\alpha(p_\rho, t_0) e^{-(\Gamma_{\text{free}}/E_\rho)(t-t_0)}. \quad (20)$$

The measured decay rate in the rest frame of the ρ meson ($E_\rho = m_\rho$) is then given by

$$\Gamma_\rho^{\text{decay}}(m_\rho^2) = \frac{f_{\rho\pi\pi}^2}{48\pi} \frac{(m_\rho^2 - 4m_\pi^2)^{3/2}}{m_\rho^2}. \quad (21)$$

Its experimental value [16] at the maximum of the resonance at $\bar{m}_\rho = 769.9 \pm 0.8$ MeV is 151.2 ± 1.2 MeV. Together with the measured value of $m_{\pi^\pm} = 139.56995 \pm 0.00035$ MeV [16] this determines the coupling constant as $f_{\rho\pi\pi} = 6.049 \pm 0.027$.

For the simulation of the collision term we need a collision criterium which involves the $\pi\pi$ -scattering cross section $\pi(p_1) + \pi(p_2) \rightarrow \rho(p_\rho)$. Assuming a Breit-Wigner mass distribution for the ρ meson

$$W(m_\rho^2) = \frac{1}{\pi} \frac{\bar{m}_\rho \Gamma(m_\rho^2)}{(\bar{m}_\rho^2 - m_\rho^2)^2 + \bar{m}_\rho^2 \Gamma^2(m_\rho^2)}, \quad \int_{4m_\pi^2}^{\infty} W(m_\rho^2) dm_\rho^2 = 1, \quad (22)$$

with a width given by the free decay rate $\Gamma_\rho^{\text{decay}}(m_\rho^2)$, Eq. (21), one gets, following standard textbook methods [17, 18],

$$\sigma(\mu_\rho^2; p_\rho, \gamma) = 4\pi s_\rho(s_\rho + 1) f^2 \frac{\mu_\rho (\mu_\rho^2 - 4\mu_\pi^2)^2}{(1 - \mu_\rho^2)^2 \mu_\rho^4 + f^2 (\mu_\rho^2 - 4\mu_\pi^2)^3} \left(1 + F_\gamma(p_1 + p_2)\right) \cdot \left[\frac{197.327 \text{ MeV}}{\bar{m}_\rho}\right]^2 \text{ fm}^2 \quad (23)$$

where

$$f = \frac{f_{\rho\pi\pi}^2}{16\pi s_\rho(s_\rho + 1)}, \quad \mu_\rho = \frac{m_\rho}{\bar{m}_\rho}, \quad \mu_\pi = \frac{m_\pi}{\bar{m}_\rho}. \quad (24)$$

Again we have summed over all three spin states of the ρ , and the factor $(1 + F_\gamma(p_1 + p_2))$ in (23) gives the Bose stimulation effect of the medium on ρ production. In an isospin symmetric system with $F_+ = F_- = F_0$ it does not depend on the final isospin state γ , but only on the momentum $p_\rho = p_1 + p_2$ of the ρ .

The cross section and decay rate in vacuum and the mass distribution are shown in Figure 1 as functions of μ_ρ .

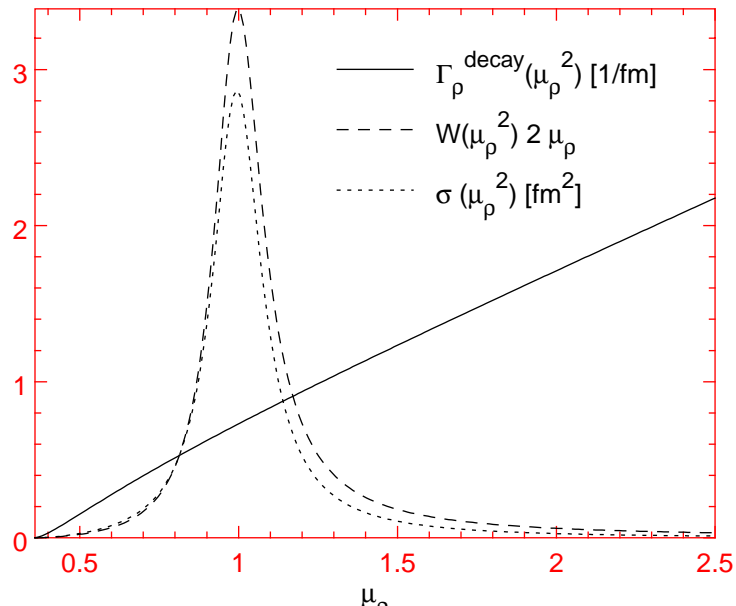


Figure 1: Free decay rate $\Gamma_\rho^{\text{decay}}(\mu_\rho^2)$, free cross section $\sigma(\mu_\rho^2)$, and Breit-Wigner mass distribution $w(\mu_\rho) = 2\mu_\rho W(\mu_\rho^2)$ for the ρ mesons as functions of their mass in units of \bar{m}_ρ , the mass at the maximum of the resonance. The position of the maxima of $\sigma(\mu_\rho)$ and $w(\mu_\rho)$ are (almost) identical, but at higher masses σ has a lower weight than $w(\mu_\rho)$.

Finally we want to note that from a formal integration of the kinetic equations over the time parameter τ it can be shown that a system with spherical symmetry in \vec{x} and \vec{p} remains spherically symmetric for all times (see Appendix A).

3 Simulation of the kinetic equations

As initial conditions for the solution of the kinetic equations we start with a system of ρ 's and π 's in global thermodynamic equilibrium at vanishing chemical potential. The thermodynamic conditions will be chosen near the expected "freeze-out" point. The particles are distributed homogeneously and isotropically in a spherical box in coordinate space with an equilibrium momentum distribution $(\exp(E/T) - 1)^{-1}$. The masses of the ρ 's are distributed with the Breit-Wigner distribution Eq. (22). For numerical reasons we will employ a cutoff for the ρ mass and for the momenta.

We assume isospin symmetry in the initial state, and since this symmetry is conserved by the strong interactions, we can exploit it to reduce the number of coupled kinetic equations to be solved. We can sum the three equations for the pion distribution functions f_α and the nine equations for the ρ meson distribution functions $F_{\alpha s}$, where $\alpha = +, -, 0$ and $s = +, -, 0$ denote isospin and spin projections, respectively. Setting $f_+ = f_- = f_0 \equiv f$ and $F_{++} = F_{+-} = \dots \equiv F$, i.e. the distributions for all isospin and spin components equal to each other, we find the two coupled equations

$$p^\mu \partial_\mu f(x, p) = -\Gamma_{\text{loss}}^\pi(x, p) f(x, p) + \Gamma_{\text{gain}}^\pi(x, p) (1 + f(x, p)), \quad (25)$$

$$p^\mu \partial_\mu F(x, p, m_\rho) = -\Gamma_{\text{loss}}^\rho(x, p, m_\rho) F(x, p, m_\rho) + \Gamma_{\text{gain}}^\rho(x, p, m_\rho) (1 + F(x, p, m_\rho)). \quad (26)$$

In the global coordinate system all distribution functions and rates are isotropic in momentum space and thus only functions of E . The rates are given by

$$\Gamma_{\text{loss}}^\pi(E) = 2 \frac{f_{\rho\pi\pi}^2}{4\pi} \int_{2m_\pi}^\infty dm_\rho w(m_\rho) \frac{\mathcal{M}}{\sqrt{E^2 - m_\pi^2}} \int_{E_-}^{E_+} dE' f(E') (1 + F(E + E', m_\rho)), \quad (27)$$

$$\Gamma_{\text{gain}}^\pi(E) = 2 \frac{f_{\rho\pi\pi}^2}{4\pi} \int_{2m_\pi}^\infty dm_\rho w(m_\rho) \frac{\mathcal{M}}{\sqrt{E^2 - m_\pi^2}} \int_{E_-}^{E_+} dE' (1 + f(E')) F(E + E', m_\rho), \quad (28)$$

$$\Gamma_{\text{loss}}^\rho(E, m_\rho) = \frac{1}{3} \frac{f_{\rho\pi\pi}^2}{4\pi} \frac{\mathcal{M}}{\sqrt{E^2 - m_\rho^2}} \int_{E_-}^{E_+} dE' (1 + f(E')) (1 + f(E - E')), \quad (29)$$

$$\Gamma_{\text{gain}}^\rho(E, m_\rho) = \frac{1}{3} \frac{f_{\rho\pi\pi}^2}{4\pi} \frac{\mathcal{M}}{\sqrt{E^2 - m_\rho^2}} \int_{E_-}^{E_+} dE' f(E') f(E - E'), \quad (30)$$

with \mathcal{M} being the spin-summed matrix element (12). The integration limits are

$$\begin{aligned} E_\pm &= \frac{1}{2m_\pi^2} \left(E(m_\rho^2 - 2m_\pi^2) \pm p m_\rho \sqrt{m_\rho^2 - 4m_\pi^2} \right), \\ E^\pm &= \frac{1}{2} \left(E \pm \frac{p}{m_\rho} \sqrt{m_\rho^2 - 4m_\pi^2} \right), \end{aligned} \quad (31)$$

and $w(m_\rho) = 2m_\rho W(m_\rho)$ is the mass distribution, Eq. (22), for the ρ mesons. The distribution functions are normalized according to

$$\begin{aligned} N_\pi = N_{\pi^+} + N_{\pi^-} + N_{\pi^0} &= 3 \int \frac{d^3r d^3p}{(2\pi)^3} f(\vec{r}, \vec{p}, t) \\ &= 3 \frac{2}{\pi} \int r^2 dr \int dE E \sqrt{E^2 - m_\pi^2} f(r, E, t), \end{aligned} \quad (32)$$

$$\begin{aligned} N_\rho = N_{\rho^+} + N_{\rho^-} + N_{\rho^0} &= 9 \int \frac{d^3r d^3p}{(2\pi)^3} \int dm_\rho w(m_\rho) F(\vec{r}, \vec{p}, m_\rho, t) \\ &= 9 \frac{2}{\pi} \int r^2 dr \int_{2m_\pi}^\infty dm_\rho w(m_\rho) \int_{m_\rho}^\infty dEE \sqrt{E^2 - m_\rho^2} F(r, E, m_\rho, t), \end{aligned} \quad (33)$$

with $N_\rho + N_\pi/2 = N$ being constant during the time evolution.

In the entropy production rate, Eq. (15), all 6 terms of the sum become equal, and it simplifies to

$$\begin{aligned} \partial^\mu S_\mu &= 6(2\pi)^4 f_{\rho\pi\pi}^2 \int dm_\rho w(m_\rho) \mathcal{M}(m_\rho) \int Dp_1 Dp_2 Dp_3 \delta(p_1 + p_2 - p_3) \\ &\quad \times \ln \left(\frac{f(p_1)f(p_2)(1 + F(p_3, m_\rho))}{(1 + f(p_1))(1 + f(p_2))F(p_3, m_\rho)} \right) \\ &\quad \times \left(f(p_1)f(p_2)(1 + F(p_3, m_\rho)) - (1 + f(p_1))(1 + f(p_2))F(p_3, m_\rho) \right). \end{aligned} \quad (34)$$

With the help of the four-dimensional δ -function the p_3 and m_ρ integrations can be evaluated. This leads to

$$\begin{aligned} \partial^\mu S_\mu &= 6\pi f_{\rho\pi\pi}^2 \int Dp_1 Dp_2 w(m_\rho) \frac{\mathcal{M}(m_\rho)}{m_\rho} \\ &\quad \times \ln \left(\frac{f(p_1)f(p_2)(1+F(p_3, m_\rho))}{(1+f(p_1))(1+f(p_2))F(p_3, m_\rho)} \right) \\ &\quad \times \left(f(p_1)f(p_2)(1+F(p_3, m_\rho)) - (1+f(p_1))(1+f(p_2))F(p_3, m_\rho) \right), \end{aligned} \quad (35)$$

with $\vec{p}_3 = \vec{p}_1 + \vec{p}_2$, $m_\rho = \sqrt{(E_1 + E_2)^2 - (\vec{p}_1 + \vec{p}_2)^2}$.

To simulate the time evolution of the particles we wrote a cascade code in which the distribution functions f and F are represented by isospin symmetric test particles. In terms of the initial radius R of the system the conserved particle number N is given by $N = \varrho \cdot R^3$, where ϱ involves the initial π and ρ densities and is a function of temperature, see Eqs. (32, 33). The initial radius of the fireball was fixed to be 5 fm; the corresponding particle numbers for temperatures $T = 100, 150$ and 200 MeV are given in Table 1.

Table 1: Particle numbers, density ϱ , and the conserved particle number N for a system of ρ mesons and pions in equilibrium at $T = 100, 150, 200$ MeV, for a fireball radius of $R = 5$ fm.

T [MeV]	N_π	N_ρ	ϱ [fm $^{-3}$]	$N = N_\pi/2 + N_\rho$
100	16.8	0.6	0.07	9
150	61.8	11.1	0.34	42
200	172.0	70.0	1.25	156

For the evaluation of the integrals over the ρ mass distribution a cutoff at $2.5 \bar{m}_\rho = 1920$ MeV was introduced, and the momentum integrals were cut off at $p_{\max} = 3.5 \bar{m}_\rho = 2689$ MeV. The mass cutoff was large enough to have no influence on our results in spite of the fact that for this cutoff the tail of the Breit-Wigner distribution still contains about 10% of the mass spectrum. The reason for this is the exponential form of the bosonic energy distribution in Eq. (33) which suppresses the formation of high-mass ρ 's and results in a deviation of the mass distribution for thermal ρ 's from the mass distribution of ρ 's at rest (see Fig. 2). Thereby the peak of the mass spectrum and its weight is shifted towards lower masses as the temperature decreases. A second peak close to the threshold of ρ production from two pions appears for temperatures below $T \approx 75$ MeV. It dominates the spectrum for low temperatures, but since we take the π 's and ρ 's to be in local equilibrium the number of ρ mesons becomes very small for these temperatures and vanishes for $T = 0$.

The code determines simultaneously the space and momentum coordinates of all test particles as functions of a global time parameter on a hyper-surface in phase space. (For an introduction to (nuclear) cascade codes see [19],[20]; the problem of a simultaneous relativistic time parameter is discussed for instance in [21], [22].) Since no mean field effects are taken into account, the particles propagate freely on straight lines between ρ formation and decay:

$$\begin{aligned} \vec{x}(\tau + \Delta\tau) &= \vec{x}(\tau) + \vec{\beta}\Delta\tau, & \vec{\beta} &= \frac{\vec{p}}{E}, \\ \vec{p}(\tau + \Delta\tau) &= \vec{p}(\tau). \end{aligned} \quad (36)$$

τ is the global time parameter.

The formation of a ρ meson in the scattering of two pions is implemented via the collision criterion

$$\pi b^2 \leq 2 \sigma(m_\rho^2, E_\rho). \quad (37)$$

The factor 2 arises from the same factor in front of the matrix element in Eqs. (27,28). $\sigma(m_\rho^2, E_\rho)$ is the medium-modified cross section (23), and b^2 is the relativistically invariant impact parameter [22]

$$b^2 = - \left(\Delta x - \frac{\Delta x \cdot P}{P^2} P \right)^2 = -(\Delta x)^2 + \frac{(\Delta x \cdot P)^2}{P^2}. \quad (38)$$

Here $P = p_1 + p_2$ is the momentum of the pion pair, and $P^2 = m_\rho^2$ is the square of their invariant mass. In the center-of-mass system of the two pions the impact parameter becomes $b^2 = \Delta \vec{x}_{\text{cm}}^2$. If b satisfies the collision criterion Eq. (37) the collision of two pions takes place in the global system at the point where their distance

$$-(\Delta x)^2 = (\Delta \vec{x})^2 = \left(\Delta \vec{x}(\tau_0) + \Delta \vec{\beta} \cdot \tau \right)^2, \quad \Delta \vec{\beta} = \frac{\vec{p}_1}{E_1} - \frac{\vec{p}_2}{E_2} \quad (39)$$

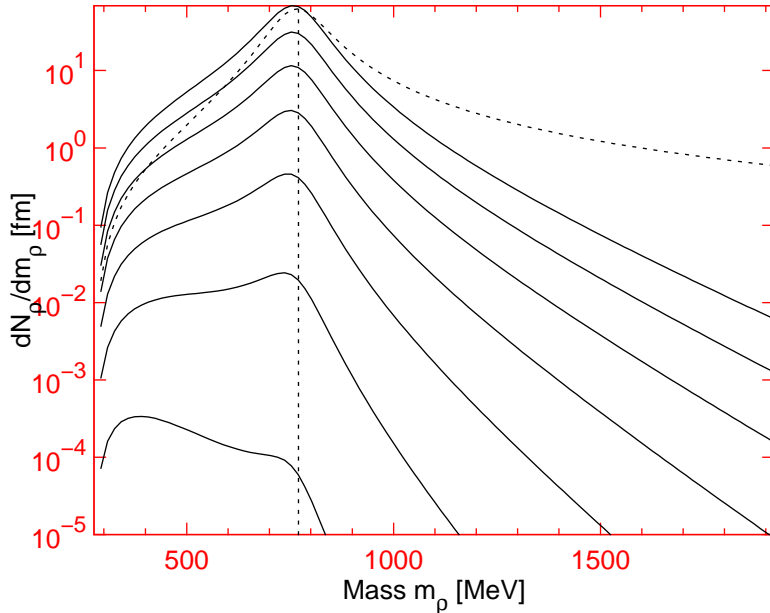


Figure 2: Mass distributions for ρ mesons in equilibrium with pions for different temperatures. The temperatures from top to bottom are $T = 200, 175, 150, 125, 100, 75$ MeV. Also shown for comparison is a pure Breit-Wigner mass distribution (dotted line), normalized at its peak to the $T = 200$ MeV curve.

is minimal. This happens at the collision time τ_c which is given by

$$\tau_c = -\frac{\Delta \vec{x}(\tau_0) \cdot \Delta \vec{\beta}}{(\Delta \beta)^2}, \quad (40)$$

and which is measured relative to the last grid point τ_0 of the global time parameter at which all trajectories were calculated.

For the decay of a ρ meson we assume isotropic decay in its rest frame. To decide if a decay in the rest frame of the ρ takes place we use the mass-dependent decay rate Eq. (18) which involves the pion distribution function in the rest frame of the decaying ρ meson. We evaluate the latter by counting pions in phase space cells around the pion momentum \vec{p} , $|\vec{p}| = \sqrt{m_\rho^2 - 4m_\pi^2}$. To avoid the transformation of all pion coordinates from the global system into the rest frame of the decaying ρ meson, we transform instead the phase space volume into the global system and do the counting there.

The phase space contributions to the cross section and decay rate are averaged over a large number of parallel ensembles. The latter influence each other only via the evaluation of the Bose factors as an ensemble average. To obtain from the discrete locations of the test particles smooth, but positive definite phase space density distributions, we smear out the contribution from a particle at some point (x, p) over phase space with a Gaussian weight function. According to the uncertainty principle the smallest possible phase space cell has the volume $\Delta^3 x \Delta^3 p = h^3$, thus the widths of the weight functions in x and p have to fulfill $\Delta x \Delta p = 2\pi\hbar$.

In evaluating the collision term, including the Bose enhancement factors, with probabilistic methods, we use a trick similar to the one described in [23] (see also [24, 25]). Instead of computing for each possible ρ decay or creation the exact contributions from the Bose factors to the decay rate and cross section, we first determine the decay or formation probability using an upper bound for the Bose factors (and thus the transition rate). Only if the collision would actually happen under these conditions, we proceed to check the collision criterium with a more realistic estimate of the Bose enhancement factors. This saves an appreciable amount of computer time by eliminating without effort a large number of “unsuccessful collision attempts”. The upper bound on the Bose factors is refined in two successive steps: In a first step we obtain a global (and time-independent) upper limit on the Bose factors from the initial phase-space density of the expanding system. If by using this global limit we find that ρ formation or decay are possible, we calculate a more accurate dynamical bound from the actual density distributions of the previous time step. Only if this second upper bound also allows ρ formation and decay do we actually calculate the distribution functions as described above.

In our simulations the number of particles in each system, $N = N_\pi/2 + N_\rho$, times the number of parallel ensembles was fixed to ≈ 300000 . We followed the system for 150 time steps of $\Delta\tau = 0.1$ fm/c.

4 Results

4.1 Decay and re-scattering rates

In general the decay of the ρ mesons is governed by the decay law

$$N_\rho(\tau + \Delta\tau) = \frac{6}{\pi} R^3 \int_{2m_\pi}^{m_{\max}} dm_\rho w(m_\rho) \int_0^{p_{\max}} dp p^2 F(E, m_\rho, \tau) e^{-\Gamma_{\text{loss}}^\rho(E, m_\rho) \Delta\tau/E}, \quad (41)$$

where $E^2 = p^2 + m_\rho^2$ and $\Gamma_{\text{loss}}^\rho$ is the loss rate for ρ mesons from Eq. (29). If we neglect the influence from Bose stimulation by surrounding pions we can replace $\Gamma_{\text{loss}}^\rho/E$ in the exponent by $\Gamma_\rho^{\text{decay}}(m_\rho)/\gamma$ from Eq. (21) where γ is the Lorentz factor between the global system and the ρ rest frame.

For the decay of ρ mesons at rest ($\gamma = 1$) into the vacuum one then obtains

$$N_\rho(\tau + \Delta\tau) = \int dm_\rho N_\rho(m_\rho, \tau) \exp(-\Gamma_\rho^{\text{decay}}(m_\rho) \Delta\tau/\gamma), \quad (42)$$

where $N_\rho(m_\rho, \tau)$ is the number of ρ mesons with mass m_ρ at time τ . Figure 3 shows a numerical simulation of this decay law with the help of our kinetic code. There is good agreement between the simulated result and the one calculated directly from Eq. (42). The striking deviation of both these results from the straight line describing the exponential decay of ρ mesons with mass $\bar{m}_\rho = 770$ MeV and a constant width $\Gamma_\rho^{\text{decay}} = 151$ MeV arises from the mass dependent decay rate (21): The heavier ρ mesons from the initial Breit-Wigner mass distribution decay first (due to their larger than average width the slope of the decay curve is at small τ actually slightly steeper than the reference line), leaving at later times only the more long lived lighter ρ mesons from the lower end of the mass distribution. Therefore the decay curve levels off at large τ .

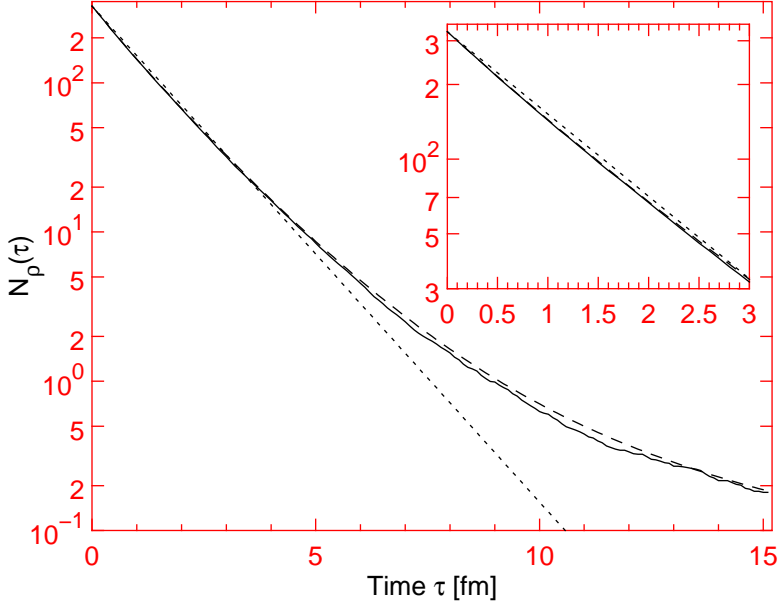


Figure 3: The number of ρ mesons as a function of time for free decay at rest simulated with 1000 parallel ensembles each containing initially 300 ρ mesons (solid) and calculated according to Eq. (42) (dashed). For comparison we show the free decay for a constant decay width $\Gamma_\rho^{\text{decay}} = 151$ MeV (dotted).

Fig. 4 shows the ρ meson decay for initially thermalized systems with different initial temperatures when we neglect the back-reaction $\pi\pi \rightarrow \rho$. One clearly sees a deviation from the just discussed decay of ρ mesons at rest, shown again by the dotted curve. A comparison between the dashed and dash-dotted curves in Fig. 4 shows that this effect is not due to medium effects via Bose stimulation from the pions in the system. It is, however, rather accurately reproduced by an analytical calculation (solid lines) which uses Eq. (41) with a thermal distribution function and again neglects Bose stimulation:

$$N_\rho(\tau + \Delta\tau) = \frac{6}{\pi} R^3 \int_{2m_\pi}^{m_{\max}} dm_\rho w(m_\rho) \int_0^{p_{\max}} dp p^2 \left[e^{\sqrt{p^2 + m_\rho^2}/T} - 1 \right]^{-1} e^{-\Gamma_\rho^{\text{decay}}(m_\rho) \Delta\tau/\gamma(p, m_\rho)}. \quad (43)$$

For all three initial temperatures the curves in Fig. 4 have approximately the same form. This was not expected, since the Lorentz-dilatation factor $\gamma(p, m_\rho) = \sqrt{p^2 + m_\rho^2}/m_\rho$ in the exponent of Eq. (43) is weighted quite differently

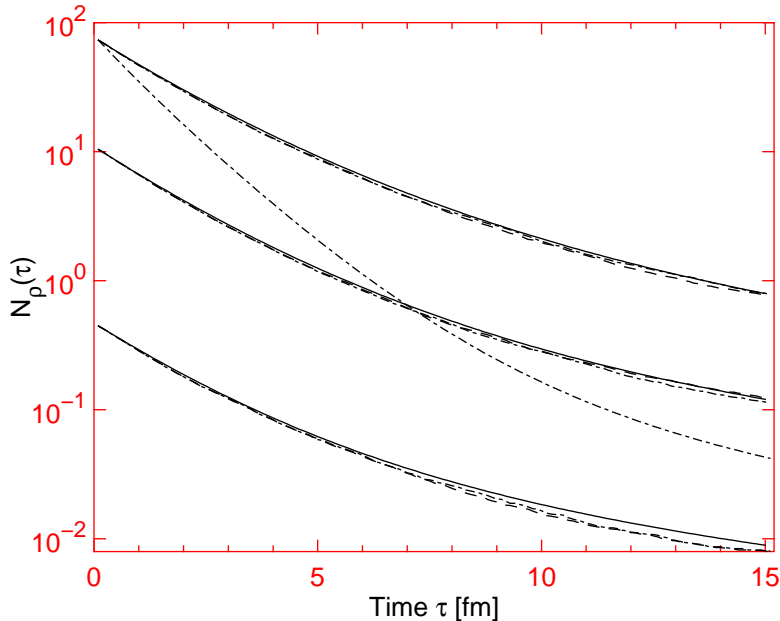


Figure 4: ρ decay for systems without ρ formation for different initial temperatures. Dashed and dashed-dotted: simulation with and without phase space contributions to the decay rate. Solid: calculated time evolution for the decay of ρ mesons with initial equilibrium distribution. From top to bottom: $T = 200, 150$ and 100 MeV. For comparison: center of mass decay (dashed-dotted) as calculated with Eq. (42) and fitted to the initial number of ρ mesons for $T = 200$ MeV.

at different temperatures, which should lead to an effectively larger decay rate at lower temperature (with smaller average $\langle \gamma \rangle$). However, at lower initial temperatures also the mass spectrum of the ρ mesons is shifted towards lower masses (see Fig. 2). Since the ρ width decreases with decreasing mass m_ρ , the net effect is a somewhat lower effective ρ meson decay rate at lower temperature.

The observed weakness of medium effects from Bose stimulation shows that the chosen initial conditions select systems which are already quite dilute in phase space. Bose statistical corrections would play a larger role if the systems were not allowed to expand [23, 24, 25].

In Fig. 5 we study the additional effects from the back-reaction $\pi\pi \rightarrow \rho$. From a formal point of view they must be included in order to preserve detailed balance and the Boltzmann H-theorem. In practice one sees that the number of resonances now decreases much more slowly (solid and dotted curves in Figs. 5a-c). Again, the inclusion of Bose enhancement factors in decay rates and scattering cross sections has no visible effect.

Another illustration of the important practical role of ρ formation by pion re-scattering is shown in Figs. 6 where the total rate for the change of the number of ρ mesons is split into its loss and gain contributions. Since the system is initialized in thermodynamic equilibrium, the two contributions should initially balance each other. That in Fig. (6) they don't quite do that is due to the fact that at $\tau = 0$ the walls around the initial sphere are removed and thus ρ mesons from the surface can now escape without re-scattering. One sees that initially the back reaction rate is still a considerable fraction of the decay rate, and that only for large times ($t \geq 5 - 10$ fm/c) the gain of ρ resonances by pion re-scattering can be neglected compared to the losses by decay. Furthermore, even if the absolute numbers for the decay and formation rates decrease drastically with decreasing temperature due to the exponentially decreasing occupancy numbers, the time dependence of the ratio between these two rates shows no strong temperature dependence.

In order to better understand these features we give in Table 2 the pion mean free path l_{free}^π for different temperatures, as extracted from the mean thermal velocity $\langle v \rangle_T$ and the effective collision time: $l_{\text{free}}^\pi = \langle v \rangle_T \tau_{\text{coll}}^\pi$. The mean thermal velocity of the pions at the beginning of the time evolution is given by

$$\langle v \rangle_T = \frac{\int_0^\infty (p/E)[e^{E/T} - 1]^{-1} p^2 dp}{\int_0^\infty [e^{E/T} - 1]^{-1} p^2 dp}. \quad (44)$$

The pion (inelastic) collision time can be calculated from ρ meson gain rate, using the conservation of $N = N_\rho + N_\pi/2$ in the process $\pi + \pi \rightarrow \rho$. Defining $\tau_{\text{coll}}^\pi = -N_\pi/\dot{N}_\pi = +N_\pi/(2\dot{N}_\rho)$ we get

$$\tau_{\text{coll}}^\pi(\tau) = \frac{N_\pi(\tau)}{2(\Delta N_{\text{gain}}^\rho(\tau)/\Delta\tau)}, \quad (45)$$

with $\Delta N_{\text{gain}}^\rho(\tau)$ taken from Figs. 6 at $\tau = 0$.

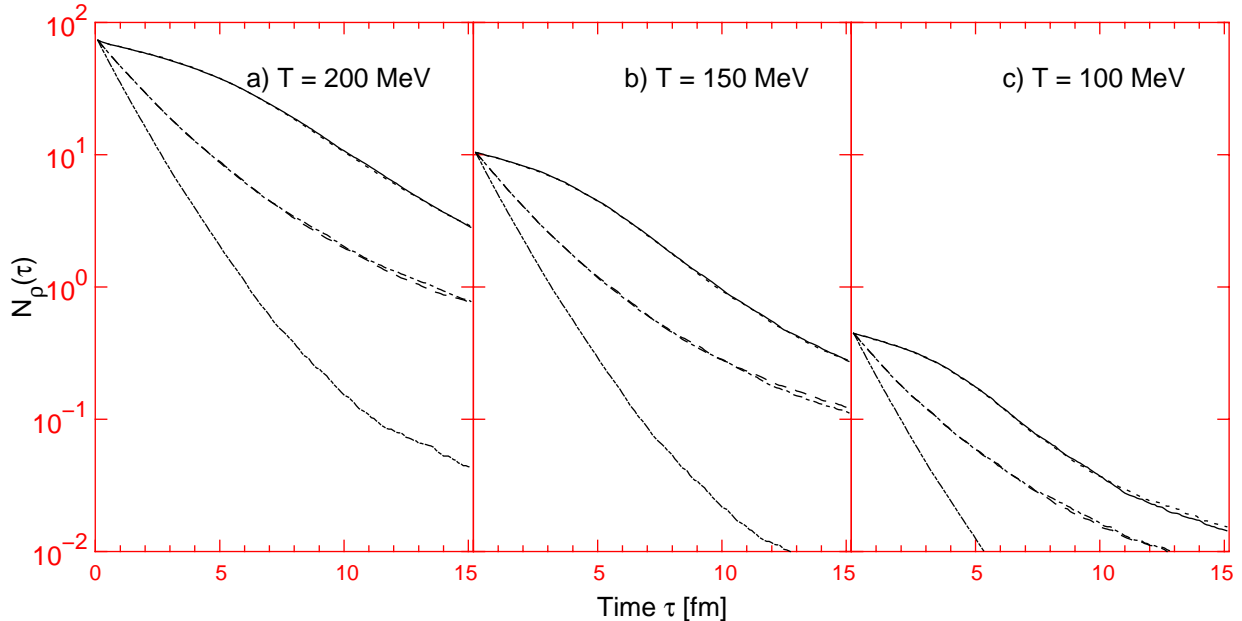


Figure 5: ρ decay from our simulation for systems with different initial temperatures. Curves from top to bottom: ρ decay plus back reaction $\pi\pi \rightarrow \rho$, with (solid) and without (dotted) Bose enhancement factors; ρ decay without back reaction, with (dashed) and without (dash-dotted) Bose enhancement factors; free decay rate ($- \cdots \cdots -$) for comparison.

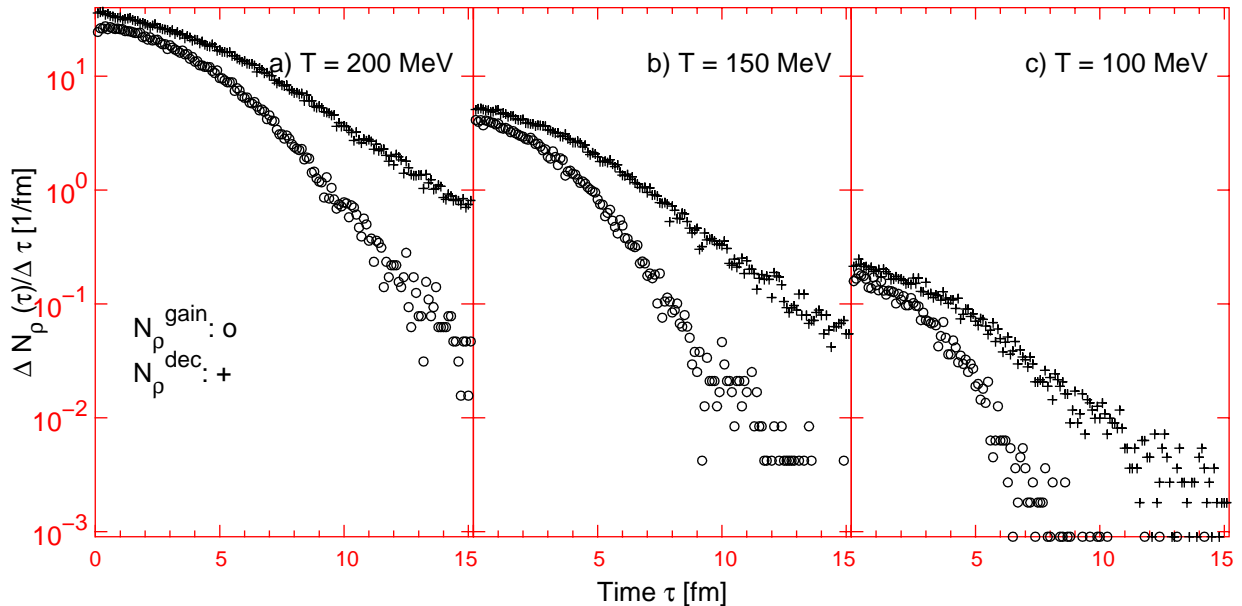


Figure 6: Gain and loss rates of ρ mesons as a function of time for different initial temperatures.

The system with $T = 100$ MeV has a pion mean free path which is much larger than the initial radius which in our simulations was chosen as $R = 5$ fm. If we assume the usual definition of “freeze out” which says, that particles will no longer hit each other if their mean free path becomes larger than the radius of the system, then “freeze out” will occur immediately after the beginning of the time evolution. In terms of absolute numbers for ρ formation (Fig. 6c) this is fulfilled to good accuracy in our simulation. On the other hand the system with $T = 200$ MeV has a pion mean free path which is smaller than the radius of the system, so that, at least at the beginning of the time evolution, it will stay close to equilibrium. Nevertheless the shape of the curves for ρ decay in Fig. 5 and for the differential gain and loss of ρ mesons in Fig. 6 are quite similar for the different temperatures, and show that the interaction itself does not change its character, only the number of particles involved gets smaller from $T = 200$ MeV to $T = 100$ MeV. Therefore “freeze out” is a quantitative statement about the number of possible interactions and not a qualitative statement about the form of the interaction.

Table 2: Collision time τ_{coll}^π , average thermal velocity $\langle v \rangle_T$, and mean free path l_{free}^π for the pions at the beginning of the kinetic evolution for different initial temperatures. The initial radius was 5 fm.

T [MeV]	τ_{coll}^π [fm/c]	$\langle v \rangle_T$	l_{free} [fm]
100	50.0	0.811	40.5
150	7.6	0.867	6.6
200	3.4	0.899	3.0

4.2 Time evolution of the ρ mass spectrum

The mass spectrum of the ρ mesons is changed both by decay and formation processes, see Fig. 7. For the decay of ρ mesons at rest and for the decay of ρ mesons with an initial thermal momentum distribution we can calculate the time evolution for the mass spectrum from Eqs. (42) and (43), respectively. The results are shown as the smooth curves in Figs. 7b,c. The temporal change of the mass spectrum arises mostly from the mass dependent decay rate. We observe that the spectra for large times become qualitatively similar in shape to the initial spectra at low temperatures (see Fig. 2) and have their peaks shifted towards the ρ formation threshold at $2m_\pi$. Comparing Figs. 7b and 7a we see that the effect of ρ formation by pion re-scattering is a reduction of the effective decay rate for the ρ mesons. If in the two different time evolutions we select points with an equal total number of ρ mesons, the *shape* of the ρ mass spectrum is, however, nearly identical.

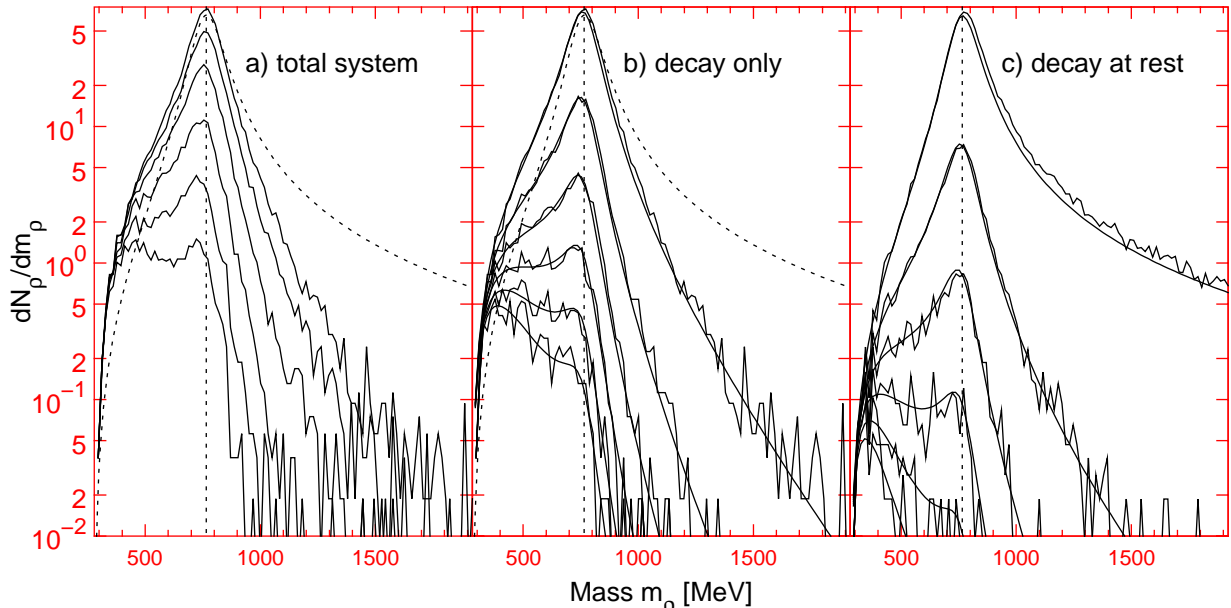


Figure 7: Mass spectrum of ρ mesons as a function of time from the kinetic simulation, for an initially thermalized system with temperature $T = 200$ MeV, in time steps of 3 fm/c. The Breit-Wigner distribution, normalized at its peak (vertical dashed line) to the initial thermally smeared mass distribution, is shown as a dotted line for comparison. **a:** total system including decays and pion re-scattering. **b:** ρ decays only, with the smooth solid curves indicating the result from Eq. (43). **c:** decay of ρ mesons at rest, with the smooth curves indicating the result from Eq. (42).

4.3 Single particle spectra

The pion spectrum from decaying ρ mesons at rest is fully determined by the initial ρ mass distribution and the two-body decay kinematics. This is shown in Fig. 8. The maximum of the pion energy spectrum at $E_\pi = \bar{m}_\rho/2 = 385$ MeV results from the maximum of the resonance at $\bar{m}_\rho = 770$ MeV,

In the absence of pion re-scattering, in our model the Lorentz-invariant pion momentum spectrum consists of a superposition of the initial thermal pion spectrum and the spectrum of decay pions from thermally distributed ρ mesons [1]. This is shown as the solid line in Fig. 9 where the contribution of pions from direct ρ decay (dotted line)

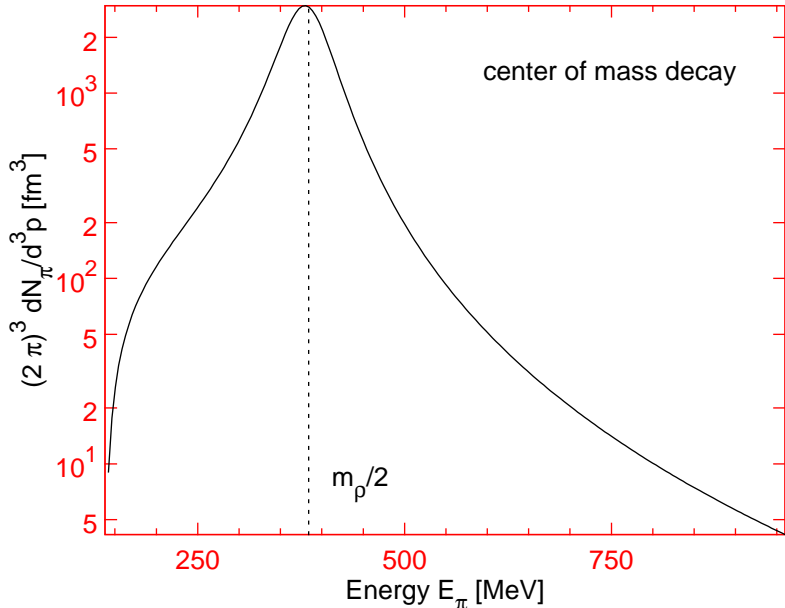


Figure 8: Energy spectrum of pions from decaying ρ mesons at rest.

is given by

$$(2\pi)^3 \frac{dN_\pi}{d^3 p} = 9 \frac{1}{p\sqrt{p^2 + m_\pi^2}} \int d^3 x \int_{2m_\pi}^{\infty} \frac{dm}{\sqrt{m^2 - 4m_\pi^2}} \int_{E^-}^{E^+} \frac{E dE}{e^{\beta E} - 1} \\ E^\pm = \frac{m^2}{2m_\pi^2} \left[\sqrt{p^2 + m_\pi^2} \pm \frac{p}{m} \sqrt{m^2 - 4m_\pi^2} \right]. \quad (46)$$

Once ρ formation by pion re-scattering is taken into account, one might expect that this changes both the direct pion spectrum (because pion loss by re-scattering into the ρ channel is not equally distributed in momentum space) and the decay spectrum from ρ decays (because the ρ 's from re-scattering pions need no longer have a thermal distribution) after the system is allowed to expand. (Of course, initially the decay and re-scattering processes don't change either spectrum because the system is in thermodynamic equilibrium.) Figs. 9 show that the continuous nature of freeze-out in our kinetic simulation has only very weak effects on the final energy spectra: even for the rather dense system with initial temperature $T = 200$ MeV the somewhat steeper final pion spectrum (compared to the initial thermal one) is very accurately described by a thermal direct pion component superimposed by decay pions from thermally distributed ρ 's. (We have checked that our simulation, with re-scattering shut off such that all ρ mesons decay directly with their initial thermal distribution, agrees with the resonance decay calculations of Eq.(46).) No additional cooling of the pions by the re-scattering processes is observed, if it is there it is accurately compensated by the developing radial collective expansion. We conclude that the calculation of the single particle spectra according to the methods used in Refs. [1, 2, 5, 6] (which do not include any kinetic evolution after the so-called freeze-out point) provides a quantitatively accurate approximation.

4.4 Entropy production during expansion

Before attempting to calculate the entropy production in our system it is very important to gain a rough qualitative picture of the phase space distributions of the particles. At the beginning the distributions in momentum and coordinate space are totally uncorrelated, due to the assumption of (global) thermal equilibrium. After allowing the system to expand, strong correlation between the momenta and coordinates develop. After a short interactive phase, the system essentially evolves by free-streaming, and after some time the momentum distribution at each point in coordinate space becomes essentially a δ -function in momentum space $\delta(r - (p/E)t)$. This very uneven distribution in phase-space leads to severe problems if one tries to calculate the entropy by a naive phase-space integration of $f \ln f$ without violating numerically Liouville's theorem that the entropy in system of free-streaming particles remains constant.

We approached this problem by a particular binning in phase space adapted to a system of free-streaming particles. We evaluated the total entropy and the entropy production rate on phase space cells of fixed size $\Delta x \cdot \Delta p = 2\pi\hbar$, whose actual shape, however, was adapted to the free expansion by projecting the particle coordinates for each time

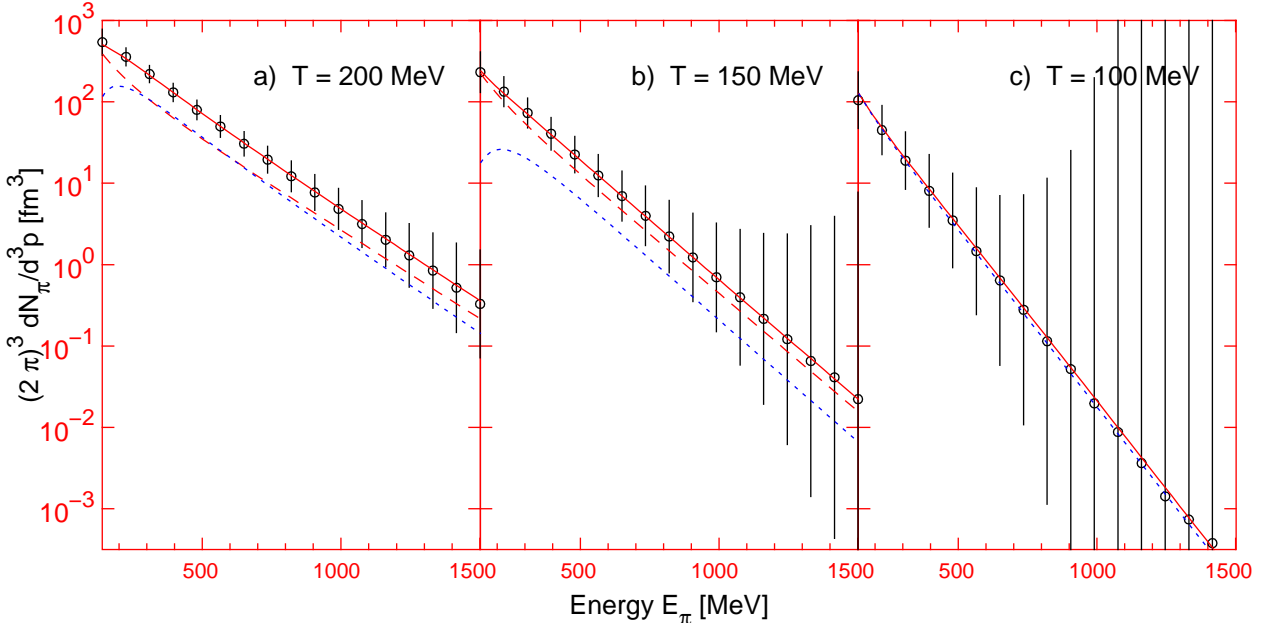


Figure 9: Pion momentum distribution as a function of pion energy in the global reference frame at the end of the time evolution. The circles indicate the results from the numerical solution, which includes both ρ decay and formation by pion re-scattering. The error bars indicate the statistical error from the sampling over parallel ensembles. For comparison: equilibrium (Bose) pion distribution at the beginning of the time-evolution (dashed line), and (as solid curve) a superposition of these initial pions with pions from ρ decays (dotted line), assuming that all initially present ρ mesons decay directly, without pion re-scattering.

step to the point in space where the particles would have started their trajectory if no interactions and decays had taken place. We then evaluated the particle densities within cubic boxes in the new coordinates, thereby obtaining an equivalent ‘‘initial’’ phase-space distribution for free streaming particles.

This method is applicable as long as only a small additional volume in phase space is occupied by particle interactions during time evolution. This is the case for systems which freeze out shortly after the beginning of the time evolution. If the system spread out more into the initially available free phase space, the phase-space densities could become too low for a reliable simulation of the kinetic equations by our test particle method.

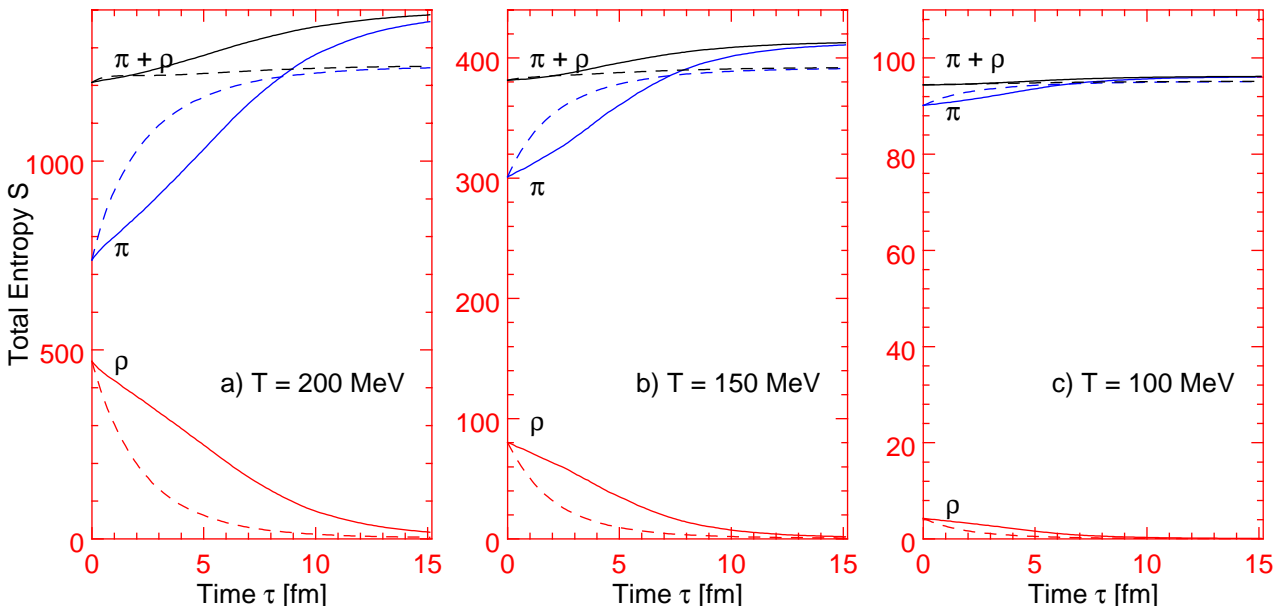


Figure 10: The total entropy as well as the individual contributions from pions and ρ mesons as a function of time. Dashed curves: ρ decay only, no pion re-scattering. Solid curves: Full numerical simulation including re-scattering processes.

In Fig. 10 we show the calculation of entropy as a function of global time τ . It is calculated from Eq. (13), by integrating the entropy current over a hyper-surface of constant global time:

$$S(\tau) = \int S^\mu(x) d\Sigma_\mu^{(\tau)}(x) = \int S^0(\mathbf{x}, \tau) d^3x. \quad (47)$$

Eq. (13) allows to separate the contributions from pions and ρ 's. The numerical simulation was stopped after $\tau = 15$ fm/c when nearly all ρ mesons had decayed and the entropy had saturated. Table 3 gives the initial equilibrium values for the entropy, Table 4 the final values and the relative increase during the time evolution, both for ρ decays without re-scattering and including re-scattering.

Table 3: Initial equilibrium values for the entropy for different initial temperatures.

T[MeV]	S_ρ	S_π	S_{tot}
200	469.8	738.4	1208.2
150	80.3	301.1	381.5
100	4.3	90.1	94.4

Table 4: Final entropy and relative entropy increase for three different initial conditions.

a) ρ decay only				
T[MeV]	S_ρ	S_π	S_{tot}	$\Delta S/S_{\text{tot}}$ in %
200	4.2	1246.8	1251.1	4
150	0.8	391.2	392.0	3
100	0.0	95.1	95.1	1
b) ρ decay plus pion re-scattering				
T[MeV]	S_ρ	S_π	S_{tot}	$\Delta S/S_{\text{tot}}$ in %
200	17.9	1369.0	1386.9	15
150	1.9	410.9	412.7	8
100	0.1	96.1	96.2	2

One sees that ρ decays alone produce very little additional entropy. Even for an initial temperature of $T = 200$ MeV, where at the beginning nearly 30% of all particles are ρ mesons (see Table 1), the total increase in entropy is only 4% of the initial value. Including the re-scattering processes leads to a somewhat larger entropy increase, by up to 15% at $T = 200$ MeV. One sees from the numbers that in general the re-scattering processes are much more efficient in producing entropy than the decays. But even at the highest temperatures investigated in this work the entropy increase is modest; for systems which are initialized near freeze-out ($T < 150$ MeV, see Table 2) it is well below 10%. This implies that, as far as calculating the entropy balance from the final particle distributions is concerned [7], the fact that freeze-out is not a sudden process can be safely ignored.

5 Conclusions

We presented a cascade simulation with thermal equilibrium initial conditions for the kinetic evolution of the π - ρ -system. This work was motivated by an earlier investigation of the influence of resonance decays on the entropy balance in relativistic heavy-ion collisions [7] which did not take into account that particle freeze-out is a continuous rather than a sudden process. We have answered the question to what extent additional entropy can be created during the final kinetic evolution between the time when local thermal equilibrium is first broken and the time when finally all resonances have decayed. We found that this additional amount of entropy is very small, less than about 10% of the entropy already present at the beginning of decoupling. We also found that this additional entropy production is dominated by the resonant re-scattering between the pions in the system rather than by the resonance decay itself. The entropy saturates once the system is so dilute that re-scattering events become unlikely.

Our simulations took into account the Bose statistics of the mesons, and we checked that our collision term satisfies Boltzmann's H-theorem and eventually leads to Bose equilibrium distributions if the matter is not allowed to expand. We realized, however, that in the calculation of the collision rates medium corrections by stimulated emission were very small. Consequently the influence of Bose statistics on the kinetics and dynamics of the expanding system turned out to be negligible.

We also found that the final pion single particle spectra resulting from the kinetic simulation can be very well approximated by the initial thermal pion distribution plus a contribution of pions from the decay of ρ mesons with a thermal momentum distribution with the same initial temperature. In other words, the modifications of the spectral shape from the final kinetic evolution of the π - ρ -system, in particular the effects of pion re-scattering into ρ -mesons, are minor. Thus the usual method [1, 2, 5] of calculating the resonance decay contributions to the pion spectrum in the “sudden approximation”, i.e. without considering the detailed kinetic balance between decays and re-scattering, is a good approximation and quantitatively quite accurate. This is certainly good news for practitioner because it means that for a thermo- and hydrodynamic analysis of measured hadron spectra the large numerical efforts of a detailed kinetic treatment of the freeze-out stage are not necessary.

In the course of our investigations we also discovered a number of other interesting aspects of our system. It is well known that in a thermalized system the ρ mass spectrum is shifted towards lower masses compared to the vacuum case, due to the weighting with the exponential thermal Bose distribution (see Eq. (33)). However, during the time evolution we observed a further downward shift in the mass peak due to the mass dependent decay rate. This effect simulates very efficiently an increasingly cooler environment for the ρ mesons as time goes on.

Acknowledgement: We thank P. Koch-Steinheimer for stimulating discussion and constructive advice during the initial stages of this work. U.H. wishes to thank B. Müller for stimulating discussions and the Physics Department at Duke University, where this work was completed, for the warm hospitality. This work was supported by DFG, GSI and BMBF.

A Appendix

For a system with spherically symmetric initial conditions in \vec{p} and \vec{x} we show by formal integration over the global time parameter τ that the kinetic equations conserve the symmetry.

From the kinetic equations we obtain formally at time $\tau + \Delta\tau$

$$F_\alpha(\tau + \Delta\tau, m_\rho) = F_\alpha(\tau, m_\rho) - (2\pi)^4 \frac{f_{\rho\pi\pi}^2}{m_\rho s_\rho(s_\rho + 1)} \sum_{\beta\gamma} \varepsilon_{\alpha\beta\gamma} \int Dp_\beta Dp_\gamma \delta(p_\beta + p_\gamma - p_\alpha) \mathcal{M} \\ \left[F_\alpha(\tau, m_\rho)(1 + f_\beta(\tau))(1 + f_\gamma(\tau)) - (1 + F_\alpha(\tau, m_\rho))f_\beta(\tau)f_\gamma(\tau) \right] \Delta\tau, \quad (48)$$

$$f_\alpha(\tau + \Delta\tau) = f_\alpha(\tau) + 2(2\pi)^4 \frac{f_{\rho\pi\pi}^2}{m_\rho} \sum_{\beta\gamma} \varepsilon_{\alpha\beta\gamma} \int Dp_\beta Dp_\gamma \delta(p_\alpha + p_\beta - p_\gamma) \mathcal{M} \\ \left[(1 + f_\alpha(\tau))(1 + f_\beta(\tau))F_\gamma(\tau, m_\rho) - f_\alpha(\tau)f_\beta(\tau)(1 + F_\gamma(\tau, m_\rho)) \right] \Delta\tau, \quad (49)$$

where $f(\tau)$ is short for $f(x(\tau), p(\tau))$ and

$$x(\tau + \Delta\tau) = x(\tau) + \frac{p(\tau)}{E} \Delta\tau \quad (50)$$

$$p(\tau + \Delta\tau) = p(\tau) + \frac{F(\tau)}{E} \Delta\tau = p(\tau). \quad (51)$$

With the above mentioned spherically symmetric initial conditions in space it follows immediately that f remains a function of only $|\vec{x}|$ for all times. To prove the same for the momentum dependence we have to show that the momentum integrations yield a result which is independent of the direction of \vec{p}_α . But the p_α -dependent distribution functions F_α , $1 + F_\alpha$ and f_α , $1 + f_\alpha$ as well as the momentum independent matrix element (12) can be pulled out of the integrals, and the remaining integrations are completely independent of p_α . Thus the spherical symmetry of the momentum distribution is also preserved.

References

- [1] J. Sollfrank, P. Koch and U. Heinz, Phys. Lett. **B252**, 256 (1990); and Z. Phys. C – Particles and Fields **52**, 593 (1991).
- [2] E. Schnedermann, J. Sollfrank and U. Heinz, in *Particle Production in Highly Excited Matter*, edited by H.H. Gutbrod and J. Rafelski (Plenum, New York, 1993), p. 175.
- [3] E. Schnedermann and U. Heinz, Phys. Rev. Lett. **69**, 2908 (1992).
- [4] E. Schnedermann and U. Heinz, Phys. Rev. **C47**, 1738 (1993).
- [5] E. Schnedermann, J. Sollfrank, and U. Heinz, Phys. Rev. **C48**, 2462 (1993).
- [6] E. Schnedermann and U. Heinz, Phys. Rev. **C50**, 1675 (1994).
- [7] J. Sollfrank and U. Heinz, Phys. Lett. **B289**, 132 (1992).
- [8] S. R. de Groot, W. A. van Leeuwen, and Ch. G. van Weert, *Relativistic Kinetic Theory* (North–Holland, Amsterdam, 1980).
- [9] S. Mrówczyński, Ann. Phys. **169**, 48 (1986).
- [10] W. Weise and T. Ericson, *Pions and Nuclei* (Clarendon Press, Oxford, 1988).
- [11] A. L. Fetter and J. D. Walecka, *Quantum Theory of Many-Particle Systems* (McGraw-Hill, New York, 1971).
- [12] Yu. M. Sinyukov, *Boson spectra and correlations in thermal locally equilibrium systems*, Kiev preprint ITP-93-8E (1993)
- [13] S. Mrówczyński and P. Danielewicz, Nucl. Phys. **B342**, 381 (1990).
- [14] C. Itzykson and J.-B. Zuber, *Quantum Field Theory* (McGraw Hill, New York, 1980), Section 3-2-3.
- [15] U. Heinz, Ann. Phys **161**, 48 (1985).
- [16] Particle Data Group, Phys. Rev. **D45** (1992).
- [17] C. Itzykson and J.-B. Zuber, *Quantum Field Theory* (McGraw Hill, New York, 1980), Appendix A-3.
- [18] H. Pilkuhn, *The Interaction of Hadrons* (North–Holland, Amsterdam, 1967).
- [19] G. F. Bertsch and S. Das Gupta, Phys. Rep. **160**, 189 (1988).
- [20] Gy. Wolf et al., Nucl. Phys. **A517**, 615 (1990).
- [21] T. Kodama et al., Phys. Rev. **C29**, 2146 (1984).
- [22] H. Sorge, H. Stöcker and W. Greiner, Ann. Phys. **192**, 266 (1989).
- [23] G. M. Welke, G. F. Bertsch, S. Boggs, and M. Prakash, *Simulation of the Boltzmann equation for bosons*, Technical Report MSUSCL-769, Michigan State University, April 1991, unpublished.
- [24] G. M. Welke and G. F. Bertsch, Phys. Rev. **C45**, 1403 (1992).
- [25] H. W. Barz, G. F. Bertsch, P. Danielewicz, H. Schulz, and G. M. Welke, Phys. Lett. **B287**, 40 (1992).